Journal of Earth & Statistics
Journal homepage: http://www.Jes.arakut.ac.ir
Doi: 10.22034/jes.2024.2028232.1046

Nature and physicochemical conditions of crystallization of biotite and plagioclase in the Zaghar intrusion(southwest of Tafarsh)

Saeed Naeemi[1], Elham shahosinie[2], Mohammad Hashem Emami[3]

[1]Department of Geology, faculty of Science, North Tehran Branch, Islamic Azad University, Tehran, Iran.
saeednaemi38@gmail.com ORCID: https://orcid.org/0000-0002-8083-9687.
[2]Ph.D. petrology, Islamic Azad University, Tehran, Iran.
[3]Associate Professor, Department of Geology, Islamic Azad University, Science and Research Branch, Tehran, Iran.

Article Info

Keywords:
Granite, Biotite, Plagioclase, Zaghar intrusion, Iran.

*Corresponding Author's Email Address:
saeednaemi38@gmail.com

Abstract

Zaghar intrusive mass is located In the 5 km west-southwest of Tafarsh city in Central Iran province.This intrusive mass is accompanied by two series of dykes. The representative samples of the intrusive mass and dikes represent the composition of diorite, quartz-diorite, monzodiorite, and granodiorite with calc-alkaline tendencies and the geochemical characteristics of I-series granitoids and M-type mantle fractions. They are also placed in the tectono-magmatic setting using the Y-Nb ratio in the range of volcanic arcs of the continental margin and at the same time as the collision. The Zaghar intrusive mass penetrated the Triassic and Cretaceous Sedimentary units and transformed them into hornfels, marble, and skarn. Consequently, the Zaghar pluton is classified as the magnetite series granitoid.

1. Introduction:

The study area is located in the coordinates of 49° 55′ to 50° 00′ longitude E to 34° 00′ to 34 41′ latitude N(fig1). The studied area is located in the central Iran zone and the structural division of Iran, this area is part of the Urmia Bazaman magmatic arc and under the Tabriz Saveh zone (Alavi, 1994). The intrusive mass was formed in the subduction zone of the continental margin. Zaghar region is mostly composed of Triassic sedimentary units, along with which Jurassic and Cretaceous sedimentary units are exposed. Besides these sediments, Eocene sedimentary volcanic units are seen, most of which are outcrops outside the study area(Hajian, 1970). A small outcrop of these units can be seen only in a part of the region. The intrusive and subvolcanic diorite-quartz diorite masses of the Oligocene have affected the Mesozoic sedimentary complex and caused proximity transformation and skarn formation in the Mesozoic sediments, especially the Triassic sediments. The age of Zaghar pluton is based on previous studies and field evidence about the disconnection of units the Eocene is attributed to the later Eocene by the dykes of this mass. Numerous dykes with trends East-West to North-East-South-West and the same composition as the diorite mass are found in the outcrop area - it is possible that some of these

dykes are older than the mass(Maleki et al., 2015). The intrusive mass contained dikes that were injected into the Cretaceous limestone and caused the formation of marble and skarn. The composition of the dike is based on the petrographic and petrology studies of diorite and granodiorite and is of subalkaline and I type magmatic series. Detailed and complete studies on the relationship between dikes and intrusive masses have not been done so far. Most of these dykes have protruding masses on the edge and roof, and the thickness of these dykes reaches up to 1 meter and their length reaches up to 311 meters.

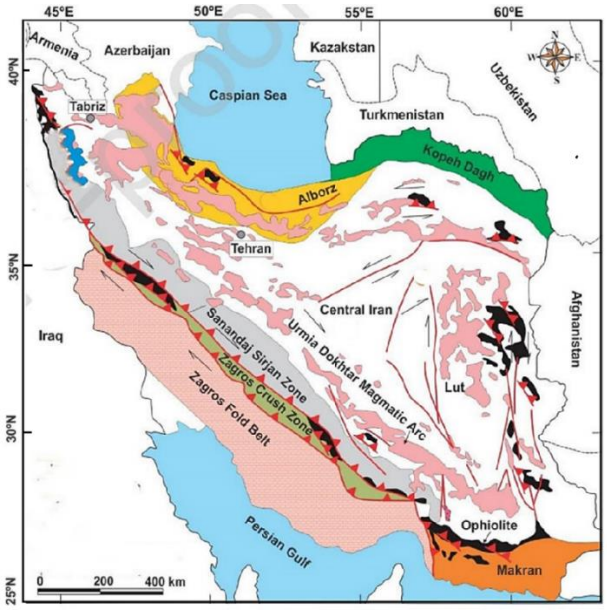

Figure 1. Simplified geological map of Iran (modified from Stocklin, 1968).

2. Study method

A total of 45 samples were taken during field works, of which 35 thin sections were prepared and studied. Thermobarometric studies were conducted on 7 thin-polished sections prepared from the granite and diorite of the study area. In this regard, amphibole, pyroxene, and plagioclase minerals were microproped through 15 point analyses. Point analyses were performed on minerals using an XPMA microprobe electron analyzer in Binalood Kansaran Iran (HORIBA Model, XGT-7200). The device operates at an accelerator voltage of 50 kV and a current intensity of 1 Am. The analyses were performed on points with a diameter of 10 μm in 8 s or each point. The structural formula was calculated using Excel spreadsheets prepared for the minerals of these rocks.

3. Petrography:

In the studied area, intrusive and semi-deep masses, with intermediate to acidic composition, have been injected and replaced in the form of stocks, dikes and numerous veins (acidic and siliceous). These masses are in Mesozoic sedimentary rocks and pyroclastic rocks - Eocene. In the vicinity of these masses, mineralized calc-silicate skarn zones have been formed. The cutting of Eocene units by the dykes of this mass is attributed to the post-Eocene period. Numerous dykes with east-west to northeast-southwest trends and the same composition as the diorite massif are exposed in the area, and it is possible that some of these dykes are old. be more than mass(Maleki et al., 2015).

-Granodiorites

These rocks are gray or greenish in color. They show granular and poikilitic textures. The main minerals in these rocks are plagioclase (~45%), quartz (~20%), K-feldspar (15-20%), and biotite (8-10%). Accessory minerals are chlorite, biotite, sericite, sphene, and clay minerals. Plagioclase is the most abundant mineral of granodiorites and the type is andesine to labradorite(in the Michel-Levy method). Some plagioclases have been altred into sericite. Quartz is subhedral with medium grain size filling the spaces between grains. Potassium feldspar of orthoclase type and some of its crystals decompose into clay minerals and sericite. Amphibole is the most abundant mafic mineral found in granodiorite with euhedral-subhedral shapes. The plagioclase minerals in this sample are generally oligoclase to andesine based on the extinction angle.

Tonalite: The mineral composition of plagioclase ranges from andesine to labradorite, and quartz is mainly seen as grains among other minerals and sometimes with wave extinction. Alkali feldspar can be seen in Orthoclase form with Carlsbad macule and sub automorph in form and perithetic. Biotites are mostly seen as sub automorph and sheet-like, and in some parts, they have been altered into chlorite. Hornblende mineral is often changed to chlorite and epidote as a secondary mineral in this rock. Alteration minerals include epidote, chlorite, sericite, and clay minerals. Apatite is often seen as very fine needle inclusions crystals in felsic minerals, especially plagioclase.The sphene mineral can be seen in both primary and secondary forms and is the result of the alteration of the ferromagnesium minerals of the rock. Zircon mineral is found in biotite and hornblende in this rock.

Quartz diorite: The composition of plagioclase in these rocks is more than that of andesine. Hornblende is seen in sub automorph form. Alteration of chlorite and epidote is evident in parts of the crystals of this mineral. Quartz makes up approximately 5 to 20% volume of the minerals in the rock. Epidote and clinozoisite along with secondary biotite and chlorite can be seen in this rock. opaque mineral is observed scattered on the surface of the sample with an abundance of 5-8%. The texture of these rocks includes granular and poikilitic.

Quartz monzonite: this sample has a granular texture and potassium feldspars are seen in it completely in the form of perthite in some places they show a myrmekite texture and the mineral composition of plagioclase is at the level of andesine. Biotite is mostly seen as sub automorphand plate-like, and in some parts, it has been altered into chlorite and sometimes sphene. Hornblende mineral is also found in this sample in the form of small grains and often altered to chlorite and epidote. Minor minerals and alterations of this rock include epidote, chlorite, sericite, and clay minerals.

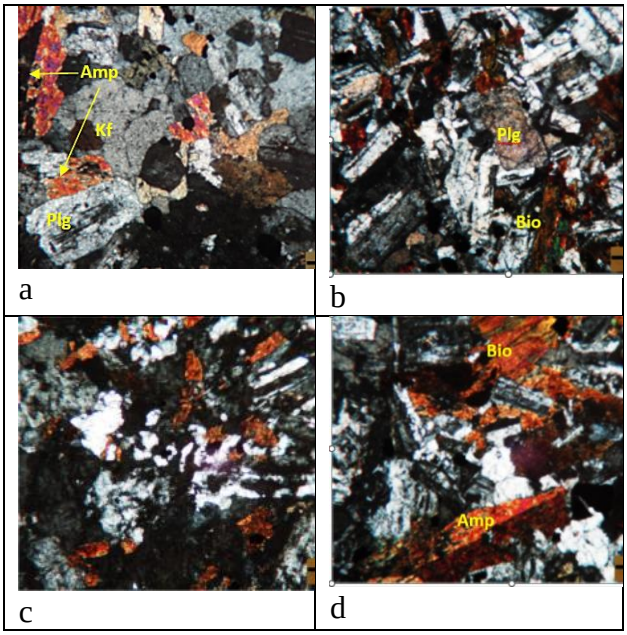

Fig 2. Photomicrographs (XPL) of mineral paragenesis: (a) abundant amphibole in the granodiorite, (b) K-feldspar crystals exhibit a perthitic texture intergrown with plagioclase and biotite in the tonalite, (c) myrmekite textures in the granite rocks. D-Presence of amphibole and biotite minerals in quartz monzonite.

4.Mineral compositions

4.1. Feldspar

Representative analyses of feldspar in the diorite, monzodiorite, and granite are shown in Table 1. On the Ab–Or–An ternary diagram (Deer et al., 1992), plagioclase compositions in the granodiorite and diorite rocks range from oligoclase to labradorite (fig 3). Using the ternary system Or-Ab-An, the temperature has been estimated from about 750 to 950 degrees Celsius for different rocks (Figure 3).

Biotite mineral chemistry

The chemical composition of magmatic biotite is sensitive to chemical and physical factors associated with the crystallization of the magma (Munoz, 1992; Abdel-Rahman, 1994 and also to exsolved hydrothermal fluids (Siahcheshm et al., 2012).

Table 1 Electron microprobe analysis of the plagioclase (wt.%).

DI: diorites. GR: Granodiorites. TA: Tonalite.
MD:Monzodiorites

GR-ZA3	MDZA3	GR-ZA2	GR-ZA1	MDZA2	TO-ZA	DI-ZA4	MDZA1	DI-ZA3	DI-ZA2	DI-ZA1	
53.928	54.409	48.572	48.882	54.693	57.363	0.025	0.015	53.411	53.447	52.72	SiO[2]
0.085	0.106	0.078	0.089	0.079	0.032	51.216	51.085	0.139	0.113	0.085	TiO[2]
28.867	28.917	32.456	32.249	28.543	26.381	0.037	0.044	30.093	30.504	30.412	Al2)O[3]
0.456	0.338	0.592	0.512	0.418	0.476	49.546	49.925	0.468	0.405	0.357	FeO
11.034	11.11	15.547	15.526	10.923	8.365	0.024	0.014	12.282	12.19	12.332	CaO
4.528	4.563	2.306	2.376	4.431	5.867	0	0.044	3.978	4.121	4.081	Na[2)O
0.399	0.389	0.141	0.169	0.53	0.489	0.011	0.004	0.405	0.269	0.268	K[2)O
0.01	0.014	0.003	0.005	0	0.027	0.458	0.449	0.026	0	0.004	MnO
0.004	0.028	0.065	0.013	0.045	0.016	0.704	0.688	0.063	0.024	0.029	MgO
9.81	9.84	8.93	8.97	9.91	10.38	0.01	0	9.61	9.58	9.53	Si
0.01	0.01	0.01	0.01	0.01	0	10.39	10.35	0.02	0.02	0.01	Ti
6.19	6.16	7.03	6.97	6.09	5.63	0.01	0.01	6.38	6.44	6.48	Al
0.07	0.05	0.09	0.08	0.06	0.07	11.18	11.25	0.07	0.06	0.05	Fe(ii)
2.15	2.15	3.06	3.05	2.12	1.62	0.01	0	2.37	2.34	2.39	Ca
1.6	1.6	0.82	0.85	1.56	2.06	0	0.02	1.39	1.43	1.43	Na
0.09	0.09	0.03	0.04	0.12	0.11	0	0	0.09	0.06	0.06	K
19.93	19.91	19.97	19.97	19.87	19.88	21.6	21.65	19.92	19.93	19.96	TOTAL
56	56.02	78.17	77.53	55.81	42.76	64.69	14.23	61.52	61.05	61.55	An
41.59	41.64	20.98	21.47	40.97	54.27	0	80.93	36.06	37.35	36.86	Ab
2.41	2.34	0.84	1	3.22	2.98	35.31	4.84	2.42	1.6	1.59	Or

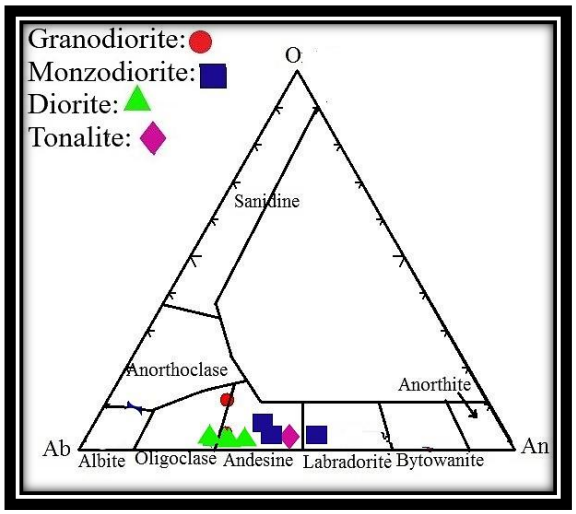

Figure 3. Compositions of feldspars of the Zaghar on the An–Ab–Or diagram (Deer et al, 1992).

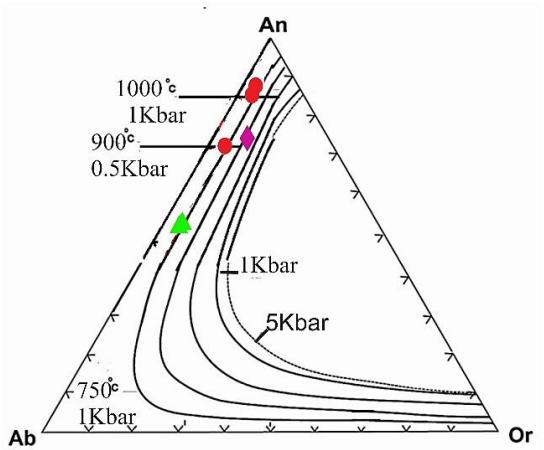

Fig 4-diagram An-Ab-Or in seck, 1971.

It is critical to be sure that the biotite grains analyzed are of primary magmatic origin, so that their chemical composition may reflect magmatic conditions of crystallization. The Ti content of biotite is thermally controlled (Patiño Douce, 1993; Stussi and Cuney, 1996). Re-equilibrated and neoformed biotite grains, resulting from low-temperature hydrothermal alteration, have less Ti than those of primary magmatic biotites. The aluminum content of biotite crystallized in equilibrium with a silicate melt reflects the peraluminosity of the melt (Stussi and Cuney, 1996) and it is commonly the host for the excess Al in peraluminous granitoids (Fleet, 2003). Therefore, biotite from the two-mica granite (Group I, whole rock aluminum saturation index > 1.1, Zhang, 2015) has higher Al (a.p.f.u > 3.1) than that of biotite from other groups (whole rock ASI < 1.1, Zhang, 2015)(Fig. 5b). In the International Mineralogical Association (IMA) classification diagram, the most of the biotites plot close to the siderophyllite-eastonite boundary (Rieder et al., 1999) with the Fe/(Fe+Mg) ratio between 0.49 and 0.74 (Fig. 5c).

Table 2 Electron microprobe analysis of the biotite(wt.%).

DI: diorites. GR: Granodiorites. TA: Tonalite.
MD:Monzodiorites

ZA-MD23	ZA-MD12	ZA-DI15	ZA-GR20	ZA-TA13	ZA-GR2	ZA-GR10	ZA-DI3	
43/15	43/15	36.04	34/44	20/93	34.82	42/21	35.73	**SiO[2]**
Mar-78	Mar-78	3.63	Feb-59	11-Apr	4.29	Mar-72	5.75	**TiO[2]**
13/45	13/45	11.79	17/65	29-Dec	10.24	25-Dec	12.33	**Al[2]O[3]**
25-Dec	25-Dec	27.62	27/37	40/79	32.73	15/55	18.22	**FeO**
0/25	0/25	0.17	0/73	0/35	0.23	0/35	0.1	**MnO**
Nov-44	Nov-44	8.21	2-Apr	Jul-32	6.39	9-Oct	11.7	**MgO**
8-Jan	8-Jan	0.05	0	0/23	0.05	0/89	0.02	**CaO**
0	0	0	0/06	Jan-94	0.04	0	0.11	**Na[2]O**
Aug-42	Aug-42	7.84	17-Oct	Nov-63	7.32	Jul-85	9.28	**K[2]O**
0	0	5.97	0	0/04	5.89	0	5.84	**Cr[2]O[3]**
0	0	2.03	0	0/01	2.04	0	2.16	**P[2]O[5]**
6/105	6/105	0.26	5/385	Mar-69	0	6/094	0.33	**Si**
1/895	1/895	0.45	2/615	Feb-55	0.55	1/906	0.69	**Al iv**
0/348	0/348	0	0/638	0/00	0	0/179	0	**Al vi**
0/402	0/402	3.82	0/305	0/54	4.63	0/404	2.43	**Ti**
0/000	0/000	0.02	0/000	0/01	0.03	0/003	0.01	**Cr**
1/449	1/449	2.03	3/579	1-Jun	1.61	1/878	2.79	**Fe**
0/030	0/030	0	0/097	0/05	0	0/043	0	**Mn**
2/413	2/413	0.01	0/937	Jan-92	0.01	2/346	0	**Mg**
0/164	0/164	0	0/000	0/04	0.01	0/138	0.03	**Ca**
0/000	0/000	1.66	0/018	0/66	1.58	0/000	1.88	**Na**
1/519	1/519	36.04	2/028	Feb-62	34.82	1/446	36.73	**K**

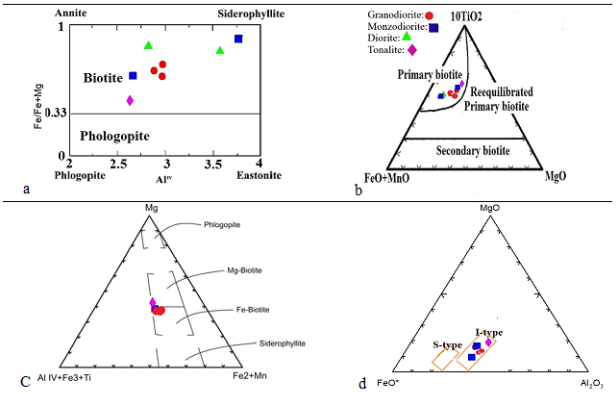

Figure 5-A- Chemical classification of mica of the studied intrusive mass (Deer et al., 1962: Speer, 1984). B- Diagram of differentiation of primary biotites, re-equilibrated, and secondary biotites (Nachite et al., 2005). C- Diagram of classification of biotites (Foster, 1960). D- Diagram of Murata and Itaya, 1987.

Chemical compositions of biotite supported this subdivision based on the different mineral assemblages. This is also supported by biotite compositions (Figure 6), which plotted in the field of biotite from calc-alkaline granitoids in the discrimination diagrams of Abdel-Rahman (Abdel-Rahman, 1994) and the subalkaline compositional field of the diagram from (Nachit et al. 1985). On the other hand, biotites from the area plutons have typical compositions of biotites from calc-alkaline granites (Fig6), supporting thus an I-type affinity. On the Fe/(Fe + Mg) vs. Al diagram, biotite grains from granite are characterized by enriched Al and Fe/(Fe + Mg) content and plotted in the I-SCR (strongly contaminated and reduced I-type) granites field(Fig. 6c).

Ishihara divided granitoid rocks into magnetite and ilmenite series. These two series are distinguished by the presence or absence of magnetite, respectively. The high ratio of Fe/Mg in biotites (Table 1) is one of the mineralogical evidence of the magnetite nature of granitoids in the region. Oxygen fugacity is the most important variable in the formation of magnetite and ilmenite granitoid. The magnetite series has higher oxygen fugacity than the ilmenite series during magma cooling (Ishihara, 1971).

Therefore, Fe in biotite in granitoids is a suitable parameter to distinguish magnetite and ilmenite series from each other. Based on this, Anderson et al., (2008) made a relative estimate of oxygen fugacity based on the FQM buffer (fayalite-quartz-magnetite) using the binary diagram of total Al (AlAV+ALVA) versus Fe# of biotites (Figure 6-a). The values of Fe# in the biotites of the region are variable (Table 1). According to the diagram in Figure 5-A, the samples of the area are in the range of magnetite granitoid and show a value of 2.6 as the AFQM average (+2.8>AFQM>+2.2).

According to the above diagram, the composition of the granite biotites of the region, with its placement in the range of magnetite granitoids, indicates the oxide conditions of this intrusive mass. The binary diagram of FeO*/FeO*+MgO versus MgO in biotites can distinguish the origin of granitoid rocks. Based on this, granitoids of crust, mantle, and crust-mantle origin are distinguished from each other (Zhou, 1986).

According to the location of the examined samples in the middle part of the diagram, it can be said that the granitoids of the region are the result of mixing magma originating from the front with the rocks of the continental crust (Fig 6b). Considering the mantle-crust origin for the mentioned mass is consistent with the magnetite series of this granitoid mass.

Ishihara (1977) states that the magnetite series granitoids occur in deeper levels (upper mantle and lower crust) compared to the ilmenite series. Coming. In the diagram of Jiang et al., 2002, the samples of the region are in the range of type I and separation of ilmenite and magnetite series granites with relative estimation of oxygen fugacity compared to FQM buffer (Ptotal=PH_2O) based on calibration (Wones, 1981).

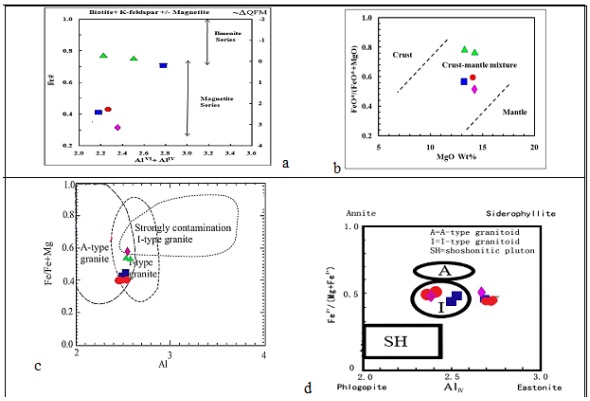

Figure 5-a- Binary diagram of total Al versus Fe# for biotites of granitoid mass Anderson et al., 2008

B- Binary diagram of FeO*/FeO*+MgO against MgO in biotites to determine the origin of granitoids. C- Al vs. Fe/(Fe + Mg) (Shabani et al., 2003) biotite composition discrimination diagrams for distinguishing the nature of the studied rocks. D- Fe^{2+}/(Mg + $Fe2^{+}$) vs. Al IV diagram for biotite in the rock granitoid (Jiang et al., 2002).

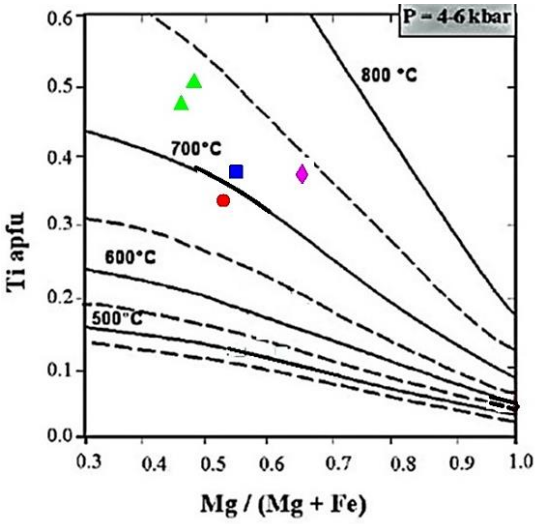

Figure 7- Geothermometry based on biotite composition (Henry et al., 2005)

Abdel-Rahman (1994) used the average (Feo*=[Feo+ (Fe_2O_3*089981/MgO)] and Al_2O_3 in different biotites as the basis of his division. He found the Feo*/MgO ratio for biotites from alkaline rocks to be 04.7, for biotites from high alumina rocks. equal to 3.84 and in calc-alkaline rocks, this ratio was determined to be 1.76 (Fig8). Calc-alkaline magmas typically form in a subduction environment. The subsolvous conditions of feldspars in calc-alkaline felsic rocks, moderate to acidic, reflect their water saturation position during their crystallization (Abdel Fattah, M., Abdel-Rahman, 1994).

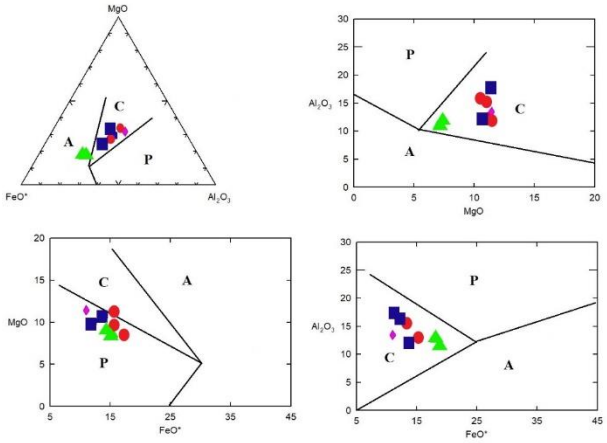

Fig 7-classification diagrams of structural setting for biotites (after Abdel-Rahman, 1994 I; field A. alkaline (mostly an orogenic extensional-related) suites including A-type granites; field C. calc-alkaline (mostly orogenic subduction-related) suites including I-type granites; field P. peraluminous rocks including collisional and S-type granites.

conclusion

The granitoid rocks of the region are located in the northwest of the central Iran zone and are calc-alkaline and I type. From a petrographic point of view lithologically., the granitoid masses of the region have a lithological composition of diorite, tonalite, granodiorite, and monzogranite. Plagioclase, albite, quartz, and orthoclase are abundant in granite rocks. These rocks show granular, myrmic, and graphic textures. According to the diagram of Deer et al. (1997), the plagioclase composition of granites is in the range of albite, oligoclase, and andesine. The composition of feldspars determined in the studied rocks by the microprob method is consistent with the results obtained from the extinction angle measurement. According to the diagram of Abdel-Rahman, 1994, granitoid

rocks are formed based on the composition of biotites in a subduction-related environment. According to the graphs of Nachite et al., (2005) and Foster, (1960), the biotites of the granitoid rocks in the study area are part of the primary and magnesium-iron-bearing biotites.

References

-Abdel Fattah, M., Abdel-Rahman, A., 1994. Nature of Biotites from Alkaline, Calc-alkaline, and Peraluminous Magmas Get access Arrow Journal of Petrology, Volume 35, Issue 2, April 1994, Pages 525–541.

-Abdel-Rahman, A.M. Nature of biotites from alkaline, calc-alkaline, and peraluminous magmas. 1994. J. Petrol., 35, 525–541.

-Abrecht, J., D.A. Hewitt, (1988), Experimental evidence on the substitution of tin in biotite, Am. Miner. 73, 1275–1284.

-Alavi, M., 1994. Tectonic of the Zagros orogenic belt of Iran: new data and interpreations", Tectonophysics.

-Anderson, J.L., Barth, A.P. and Mazdab, J.L.W.F., 2008. Thermometers and thermobarometers in granitic systems, Reviews in Mineralogy and Geochemistry, 69 (1), 121-142.

-Arima, M. and Edgar, A.D., 1981. Substitution mechanisms and solubility of titanium in phlogopites from rocks of probable mantle origin. Contributions to Mineralogy and Petrology, 77, 288–295.

-Fleet, M.E., 2003. Rock-Forming minerals, 2nd edition. Volume 3A: Micas. The Geological Society of London, pp. 325-585.

-Foster, M. D., 1960. Interpretation of Composition of Trioctahedral Micas. Geological Survey Professional Paper, 354B: 1–49.

-Hajian, Javad., 1970. Geology of Tafarsh, Organization of Geology and Mineral Exploration of Iran, Report No. 82

-Henry, Darrell J., Charles V. Guidotti, and Jennifer A. Thomson. 2005. The Ti-saturation surface for low-to-medium pressure metapelitic biotites: Implications for geothermometry and Tisubstitution mechanisms." American Mineralogist 90 (2005) 316-328.

-Ishihara, S., 1971. Major molybdenum deposits and related granitic rocks in Japan, Rep. Geol. Surv. Japan, 239, 1-178.

-Ishihara, S., 1977. The magnetite-series and ilmenite-series granitic rocks, Mining geology, 27 (145), 293-305.

-Jiang, Y.H., Jiang, S.Y., Ling, H.F., Zhou, X.R., Rui, X.J. and Yang, W.Z., 2002. Petrology and geochemistry of shoshonitic plutons from the western Kunlun orogenic belt, Xinjiang, northwestern China: implications for granitoid geneses, Lithos, 63(3-4, 165-187).

-Malki, E., Ghadimi, F., Ghomi, M., 2015. Geology, mineralogy, geochemistry and zonation of the Au skarn in Tafrash Zaghar. Thesis Submitted in Partial Fulfillment of the Requirements for the Degree of Master of Science. Arak University of Technology. 140P.

-Munoz, J.A., 1992. Evolution of a continental collision belt: ECORS-Pyrenees crustal balanced cross-section. Thrust Tectonics, 235–246

-Murata, M., Itaya, T., (1987). Sulfide and oxide minerals from S-type and I-type granitic rocks, Geochiemica et Cosmochimica Acta v.51, pp.497-507.

-Nachit, H.; Razafimahefa, N.; Stussi, J.M.; Carron, J.P. 1985. Composition chimique des biotites et typologie magmatique des granites. C.R. Acad. Sci. Paris, 301, 813–818.

-Patino Douce, A., Beard, J.S., 1995. Dehydration-melting of biotite and quartz amphibolites from 3 to 15 kb. Jouranal of Petrology 36, 707-738.

-Rieder, M., Cavazzini, G., D'yakonov, Y. S., et al., 1999. Nomenclature of the Micas. Mineralogical Magazine, 63(2): 267 – 279.

-Robert J.L., 1976. Titanium solubility in synthetic phlogopite solidsolutions, Chem. Geol. 17 213–227.

-Seck, H.A. 1971. Koexistierende Alkalifeldspate and Plagioklase in System NaAlSi3O8 KAlSi3O8-CaAl2Si2O8 bei Temperaturen 650 c bis 900 c. Neues Jahrbuch für Mineralogie Abhandlungen, 115, 315-345.

-Siahcheshm, K., Calagari, A.A., Abedini, A., Lentz, D.R., 2012. Halogen signatures of biotites from the Maher-Abad porphyry copper deposit, Iran: characterization of volatiles in syn- to post-magmatic hydrothermal fluids. Int. Geol. Rev. 54, 1368-1353.

-Speer, J, A., 1984. Mica in igneous rock In: Micas Bailey, S. W.(Eds): Mineralogical Society of America Review in Mineralogy 13:299-356.

-Stocklin, J., 1968. Structural History and Tectonic of Iran: A Review. American Association of Petroleum Geologists Bulletin, USA, 52, 1229-1258.

-Stussi, J.M., Cuney, M., 1996. Nature of biotites from alkaline, calc-alkaline and per-aluminous magmas by Abdel-Fattah M. Abdel-Rahman: a comment. J. Petrol. 37,1025–1029.

-Tronnes, R.G., Edgar, A.D., and Arima, M. (1985) A high pressure-high tempera-ture study of TiO2 solubility in Mg-rich phlogopite: Implications to phlogopite chemistry. Geochimica et Cosmochimica Acta, 49, 2323–2329.
-Uchida E., Endo S., Makino M., 2007. Relationship between solidification depth of granitic rocks and formation of hydrothermal ore deposits". Resource Geology 57; 47-56.
-Wones D. R. and Eugster H.P., 1965, Stability of biotite: experiment, theory, and application. American Mineralogist, 50, 1228-1272.
-Wones, D.R., 1981. Mafic silicates as indicators of intensive variables in granitic magmas, Mining Geology, 31(168), 191-212.
-Zhou, Z. X., 1986. The origin of intrusive mass in Fengshandong, Hubei province, Acta Petrologica Sinica, 1, 007.
-Zhang. W., 2015. Petrological and metallogenic studies of the Nashwaak Granite and felsic dykes associated with the Sisson Brook W-Mo-Cu deposit, west-central New Brunswick, Canada. Ph. D. Thesis, unpublished.